Interaction of Hoechst 33258 and Ethidium with Histone1−DNA Condensates

Rupa Sarkar and Samir Kumar Pal*

Unit for Nano Science & Technology, Department of Chemical, Biological & Macromolecular Sciences, S. N. Bose National Centre for Basic Sciences, Block JD, Sector III, Salt Lake, Kolkata 700 098, India

Received April 6, 2007

We report structural and dynamical aspects of DNAs from various sources including synthetic oligonucleotides in bulk buffer and as a complex with histone1 (H1). High-resolution transmission electron microscopic (HRTEM) studies reveal the structural change of the DNAs upon complexation with H1 leading to formation of compact-globular and hollow-toroidal particles. In order to explore the functionality of ligand binding of the DNAs and their complexes with H1, we have used two biologically common fluorescent probes Hoechst 33258 (H33258) and Ethidium (EB) as model ligands. Picosecond resolved fluorescence and polarization gated anisotropy studies examined that the minor groove binding of H33258 to the genomic DNA−H1 complex remains almost unaltered. However, the intercalative interaction of EB with the DNA in the complex is severely perturbed compared to that with the DNA in bulk buffer. Time-dependent solvochromic effect of the probe H33258 further elucidates the dynamical solvation, which is reflective of the overall environmental relaxation of the DNAs upon condensation by H1. We have also performed circular dichroism (CD) studies on the DNAs and their complexes with H1, which reveal the change in conformation of the DNAs in the complexes. Our studies in the ligand-binding mechanisms of the DNA−H1 complex are important to understand the mechanism of drug binding to linker DNA in condensed chromatin.

Introduction

DNA is highly condensed within living cells as compared to free DNA in solution.[1] The condensation of free DNA in vitro has long been of interest as a potential model for DNA condensation in vivo.[2,3] Recently, compaction of DNA has attracted much attention for its direct relevance to the DNA delivery as a part of gene therapies.[4,5] In a typical eukaryotic cell, over 1 meter of DNA resides in a nucleus in condensed form, which has a diameter of approximately 10 μm. Earlier, detail structural studies on the DNA condensates in presence of H1 by using circular dichroism (CD) spectroscopy have been progressed in the literatures.[6−8] Molecular recognition of a DNA condensate by small ligands is also important in order to understand the binding of drug molecules in the physiologically relevant form of the DNA. Early studies in the literature have used ethidium (EB) as a model intercalator ligand to study the nature of ligand binding in the condensed form of DNA.[9,10] A recent study[11] from our group reveals that the binding of EB to a genomic DNA is severely perturbed in the condensed form of the DNA compared to that in bulk buffer. Another way of DNA-recognition by small ligands is through non-covalent minor-groove binding. It is well-known that a number of ligands including several anti-cancer drugs[12,13] interact with DNA molecules through the minor-grooves. However, to date, a detail study on the nature of ligand binding in the minor groove of a DNA upon condensation by H1 is lacking in the literature.

In this study, we use two genomic DNAs extracted from calf thymus and salmon testes to examine their structural and functional aspects upon complexation with the linker histone H1. High-resolution transmission electron microscopy (HRTEM) and circular dichroism (CD) spectroscopy are used for the structural investigation of the complexes. In order to explore the nature of ligand-binding of the complexes, two biologically common fluorescent probes, Hoechst 33258 (H33258) and Ethidium (EB; Scheme 1) are used as model ligands. H33258 is well-known to be one of the potential minor groove binders.[14−16] The solvochromic property[17] of the probe H33258 offers a unique opportunity to study the change in polarity of the DNA minor groove upon complexation with H1. The cationic EB, one of the most popular DNA probes,[9,11] intercalates into the base pairs of the DNA molecules and reports its structural change.[10,11] In order to study the perturbation of the intercalative ligand binding of the condensed DNAs as reported in the earlier,[11,18] we have also investigated the nature of EB binding in our DNA−H1 condensates.

The structural and functional aspects of small synthetic oligonucleotides of known sequences [GCGAAATTTCGC, duplex1 and GCGCGCGCGCGC, duplex2] upon complexation with H1 have also been explored. The specific sequence of duplex1 is shown to recognize H33258 in a very specific manner (in the AT tract) through minor groove binding.[14,19] By observing picosecond to nanosecond dynamics of population and polarization-analyzed anisotropy of the probe H33258 upon UV excitation, we elucidate the nature of local solvation, polarity, and binding rigidity of the probe in DNA and DNA-H1 complex. On the other hand poly GC sequence of duplex2 is ideal for the intercalative mode of EB-binding.[20] The significant change in the fluorescence intensity and lifetime of the probe EB upon binding to DNA and DNA−H1 complex clearly explore the perturbation of intercalative interaction of the ligand in the DNA condensate.

* Corresponding author. E-mail: skpal@bose.res.in. Fax: 91 33 2335 3477.

10.1021/bm700690p CCC: $37.00
Published on Web 09/29/2007

Scheme 1. Molecular Structures of the DNA Binding Ligands (a) Hoechst (H33258) and (b) Ethidium Bromide (EB)

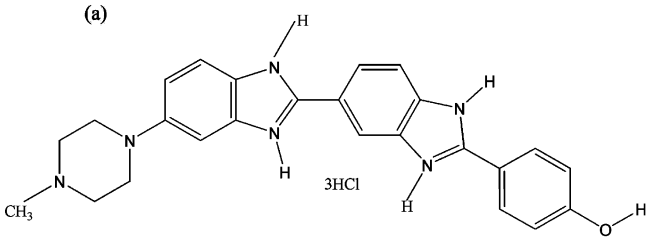

Hoechst 33258 (H33258)

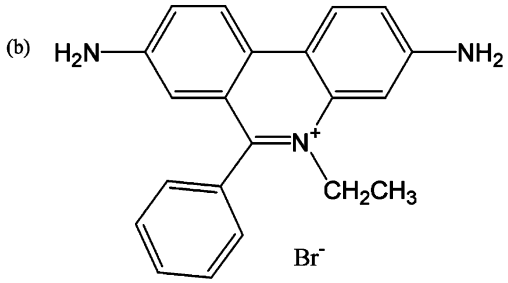

Ethidium Bromide (EB)

Materials and Methods

Chemicals are obtained from the following sources: DNA from calf thymus and salmon sperm (Sigma), calf thymus histone 1 (H1; Sigma), H33258 (Molecular Probes), and EB (Molecular Probes). The chemicals are of highest commercially available purity and used as received. In order to check the purity (contaminations by amino acid and peptides) of the commercially available genomic DNAs, absorption spectra of genomic DNAs are measured. For the DNAs from calf thymus and salmon sperm, the absorption ratios of 260 nm/280 nm give values of 1.85 and 1.90, respectively, indicating highly purified preparations of the DNAs.[21,22] The purified (reverse phase cartridge) synthetic DNA oligonucleotides of 12 bases (dodecamer) with sequences GCGCGCGCGCGC and CGCAAATTTGCG are obtained from Gene Link. In order to reassociate the single strand DNA into self-complimentary ds-DNA [$(CGCAAATTTGCG)_2$, duplex1 and $(GCGCGCGCGCGC)_2$, duplex2], thermal annealing is performed as per the methodology prescribed by the vendor. The aqueous solutions of the oligonucleotides are dialyzed exhaustively against Millipore water prior to further use. It has been noted that bindings of H33258 and EB to the oligonucleotides depend upon the ionic strength of the host solution. Aqueous sample solutions of genomic DNAs are prepared in 50 mM phosphate buffer of pH 7.

The procedure for preparing genomic DNA aqueous solutions is similar to that in refs 21 and 22. In the present study, the concentration of base pairs of a DNA is considered as the overall concentration of the DNA. The nucleotide concentrations are determined by absorption spectroscopy using the average extinction coefficient per nucleotide of the DNA (6600 $M^{-1}cm^{-1}$ at 260 nm).[22] The final DNA base pair concentration is 50 μM in all sample solutions. In order to avoid dimerization, H33258 and EB concentrations are maintained at 0.5 and 1 μM, respectively. Ligand−DNA complexes are prepared by dropwise addition of the probe solutions (H33258 or EB) to the DNA solutions with continuous stirring and the final solutions are allowed to equilibrate for half an hour. DNA−H1 complexes are obtained by dropwise addition of H1 solution to the pre-equilibrated solutions of ligand−DNA with vigorous stirring. In our studies, 5 and 30 μM H1 concentrations are used to prepare genomic and synthesized DNA−H1 complexes, respectively. By observing the relative percentage of the bound ligands (EB and H33258) from the fluorescence transients and rotational anisotropy studies on the ligand−DNA complexes, we calculate the binding constant (K) of the ligand H33258 and EB with

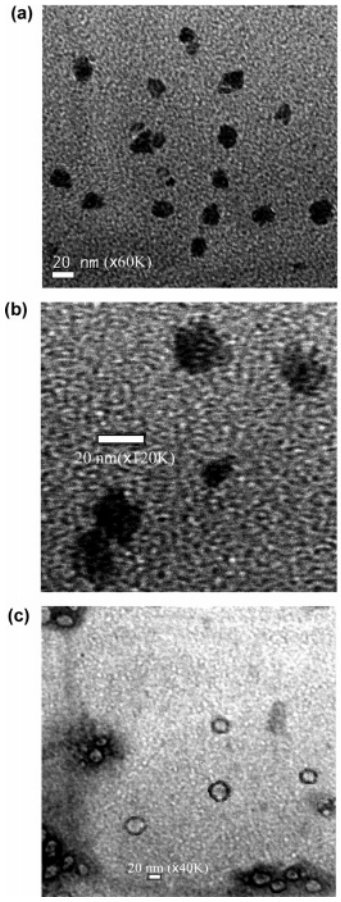

Figure 1. High-resolution transmission electron micrographs (HR-TEM) of (a) calf thymus DNA condensate (×60K), (b) calf thymus DNA condensate (×200K), and (c) toroidal form of salmon sperm DNA condensate (×40K) are shown. The DNA concentration is maintained at 10 μg/mL.

the DNA in the sample by using following equation:

$$K = \left[\frac{[\text{ligand}-\text{DNA}]}{([\text{ligand}] - [\text{ligand}-\text{DNA}])\times([\text{DNA}] - [\text{ligand}-\text{DNA}])}\right] \quad (1)$$

Steady-state absorption and emission are measured with a Shimadzu UV-2450 spectrophotometer and a Jobin Yvon Fluoromax-3 fluorimeter, respectively. Circular dichroism (CD) spectra are taken in a Jasco-815 spectropolarimeter using a quartz cell with a path length of 0.2 cm. High-resolution transmission electron microscopy (HRTEM) imaging is performed with a JEOL (JEM-2100) electron microscope at IIT-KGP, India. To prepare TEM samples carbon-coated copper grids are stained by 2% (w/v) uranyl acetate solution. Finally, samples are prepared by placing a drop of the desired filtered solutions on the stained grids and are allowed to evaporate overnight at room temperature. Particle size is determined from the TEM images using an operating voltage of 100 kV. All fluorescence decays are taken by using the picosecond-resolved time correlated single photon counting (TCSPC) technique. The commercially available setup is apicosecond diode laser pumped time-resolved fluorescence spectrophotometer from Edinburgh Instruments, U.K. To excite EB and H33258, picosecond excitation pulses from diode lasers with excitation wavelengths of 409 and 375 nm (instrument response function, IRF = 80 ps), respectively, are used. Fluorescence from the samples was detected by a microchannel plate photomultiplier tube (MCP-PMT, Hammamatsu) after dispersion through a grating monochromator. For all decays the polarizer in the emission side is adjusted to be at 54.7° (magic angle) with respect to the polarization axis of the excitation beam.

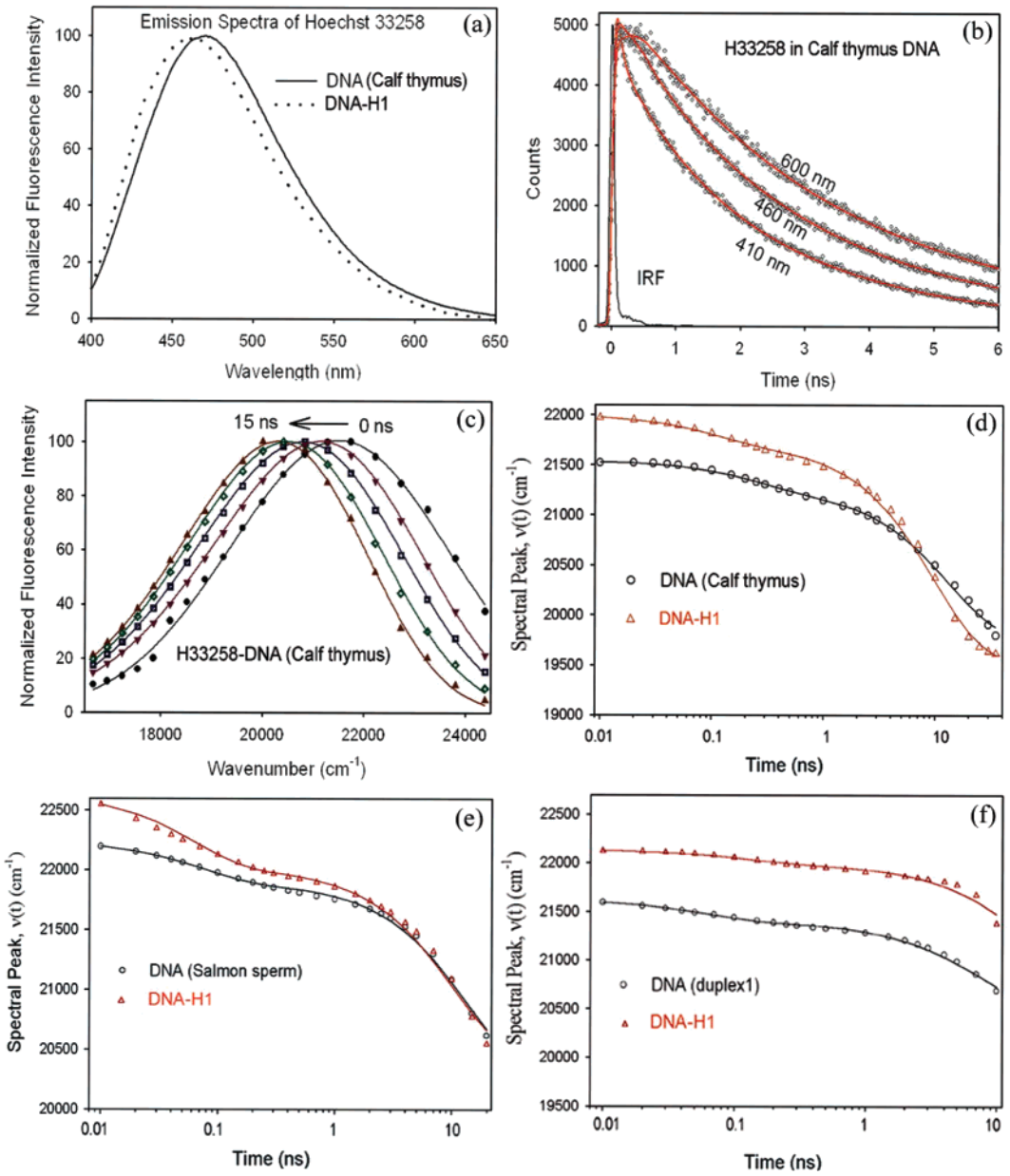

Figure 2. (a) Steady-state emission spectra of H33258 in calf thymus DNA and the DNA−H1 complex (b) Fluorescence transients of H33258−calf thymus DNA at three different detection wavelengths. (c) Time-resolved emission spectra of H33258 in calf thymus DNA. Time-resolved fluorescence spectral peak frequency of H33258 in (d) calf thymus DNA and DNA−H1 complex, (e) salmon sperm DNA and its condensate, and (f) duplex1 and duplex1−H1 complex are shown. Solid lines indicate biexponential numerical fitting of the experimental data points.

To construct time-resolved emission spectra (TRES), we follow the technique described in refs 23 and 24. The time dependent fluorescence Stoke's shifts, as estimated from TRES, are used to construct the normalized spectral shift correlation function or the solvent correlation function $C(t)$ defined as,

$$C(t) = \frac{\nu(t) - \nu(\infty)}{\nu(0) - \nu(\infty)} \tag{2}$$

where $\nu(0)$, $\nu(t)$, and $\nu(\infty)$ are the emission maxima (in cm^{-1}) at time 0, t, and ∞, respectively. The $\nu(\infty)$ values have been taken to be the emission frequency beyond which insignificant or no spectral shift is observed. The $C(t)$ function represents the temporal response of the solvent relaxation process, as occurs around the probe following its photoexcitation and the associated change in the dipole moment. For anisotropy ($r(t)$) measurements, emission polarization is adjusted to be parallel (I_{para} = fluorescence intensity at parallel polarization) or perpendicular (I_{perp} = fluorescence intensity at perpendicular polarization) to that of the excitation and the anisotropy is defined as,

$$r(t) = \frac{[I_{para} - GI_{perp}]}{[I_{para} + 2GI_{perp}]} \tag{3}$$

G, the grating factor is determined following longtime tail matching technique[25] to be 1.1.

Results and Discussion

1. Structure of Genomic DNA Condensates. The complexes of calf thymus DNA with H1 are shown in Figure 1a,b with different resolutions. The TEM images show compact-globular complexes of average diameter of 20 ± 2 nm. The high-resolution image (Figure 1b) rules out the existence of void-like space in the complex. In contrast, TEM images of salmon sperm DNA condensates with H1 (from calf thymus) show

toroid-type particles with central holes (Figure 1c). It should be noted that the difference in the structure of the complex of calf thymus DNA with H1 from that of the salmon sperm DNA is not due to the impurity (protein dirt) present in the genomic DNAs. As discussed earlier, the absorption spectroscopic studies on the DNAs are consistent with their highly purified form. It should be noted that toroidal DNA condensates are the natural morphology of DNA packaged within vertibrate sperm cells.[26] Another fact that the compact nature of the calf thymus DNA-H1 complex (DNA and protein are from same species; intraspecies) compared to that of the salmon sperm DNA−H1 (interspecies) may be due to the greater compactness of intraspecies DNA condensates than that of the interspecies DNA condensates. In our TEM experiments on the salmon sperm DNA−H1 complex, we have found the toroid diameter and hole-diameter to be 29 ± 2 and 25 ± 4 nm, respectively. Cryoelectron microscopic characterization[27] on spermine induced DNA compaction shows formation of C-type toroid with a central hole diameter of 15−40 nm and an external diameter of 50−110 nm. Our observation of ∼30 nm toroid diameter of salmon sperm DNA of reported length of 2000 base pairs[28] is well within statistical limit.[29] For much longer DNA with lengths of 60 000 base pairs, the toroid diameter is reported to be 90 nm.[26]

2. Ligand Binding to DNA. *A. Minor Groove Binding.* In this study, we use H33258, which displays sequence specificity, preferentially binds to the AATT stretch of DNA double helix,[14,19] and exhibits a Stokes shift that heavily depends upon solvent polarity of the host environment.[17] It is reported that the interaction of H33258 may lead to DNA condensation at higher concentrations of the probe ([probe]:[DNA base] = 2.50:1).[30] However, in our studies, the possibility of the DNA condensation by the probe molecules can be ruled out as the samples contain [probe]:[DNA base] = 1:200. It is well-known that[15,31] the dynamical nature of DNA is important for its recognition by small molecules and by proteins. The local internal relaxation dynamics of DNA on the picosecond to nanosecond time scale is addressed in a series of publications from Berg's group.[32−36] In the studies, one coumarin chromophore (coumarin-102 deoxyriboside) is incorporated into an oligonucleotide where it replaces a native base. The measured solvation dynamics of the probe using time-resolved stokes shift technique reveals two relaxation time constants of 300 ps (47%) and 13 ns (53%).[32] The effect of counterion motion to the interior dynamics of DNA has also been described on that time window.[34] However, the fate of water molecules/counterions at the surface of a DNA, particularly solvation relaxation in the minor groove upon complexation with the protein H1 is yet to be explored. This is important as solvation in the minor groove of B-DNA has a significant role to maintain the structural integrity of DNA compared to that in the major groove.[37]

Figure 2a shows the emission spectra of the probe H33258 in the calf thymus DNA and DNA−H1 complex. In hydrophobic environments the dye shows blue shift.[16] The emission maxima of the ligand in buffer and in DNA are 515 and 470 nm, respectively.[15] The ligand bound to the DNA−H1 complex shows an emission maximum at 460 nm indicating more nonpolar environment of the probe in the DNA upon complexation with H1. The fluorescence transients of H33258-calf thymus DNA in buffer at three characteristic wavelengths are shown in Figure 2b. The numerical fittings (solid lines) of the data are made up to 35 ns. However, in order to show the change in the transient in the blue side of the emission spectra from that in the red side, we have shown the data up to 6 ns. The transients with a systematic series of wavelength detection from

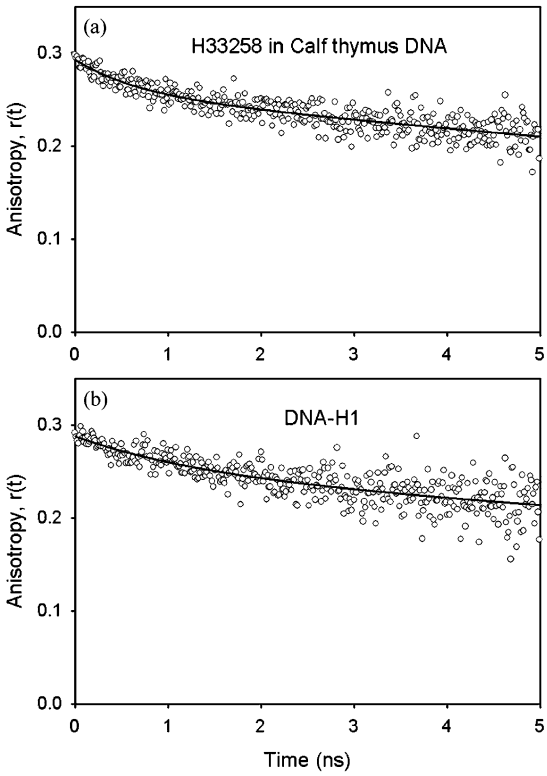

Figure 3. Time-resolved fluorescence anisotropy of H33258 in calf thymus DNA (a) and its condensate (b) Solid lines indicate biexponential numerical fitting of the experimental data points.

410 to 600 nm with a 10 nm regular wavelength interval show three distinct time scales of ∼150 ps, ∼2.2 ns, and ∼4 ns. The blue wavelength (410 nm) decays with 150 ps time constant and rises with a similar time constant at the red side (600 nm), which is the signature of solvation dynamics.[38−40] Other two time constants remain similar in all of the wavelengths of detection. Time-resolved emission spectra (TRES) of the H33258−calf thymus DNA complex up to 15 ns is shown in Figure 2c. The net spectral shift is 1715 cm^{-1} (from 21 514 to 19 799 cm^{-1} in 35 ns). It should be noted that the emission peak of H33258 in nonpolar dioxane is 22 935 cm^{-1}.[15] The difference of the peak value of H33258 in DNA environments at $t = 0$ from that of the peak in the nonpolar medium reflects the missing dynamics of the corresponding environments within our instrumental resolution.[41] The nature of solvent correlation function, $C(t)$, from the temporal spectral shift as reported in our previous work[16] reveals similar results. Figure 2d demonstrates that the time evolution of the spectral peak frequency of H33258 attached to calf thymus DNA and in the DNA−H1 complex. The data points are fitted with a biexponential decay function yielding different solvent relaxation time constants for the DNA in different environments. The dynamics of the H33258−calf thymus DNA complex shows two distinct time constants of 250 ps and 13.50 ns. The time scales obtained from our experiment are similar to the relaxation times seen in the coumarin modified DNA.[32] The time constants are much slower than the low-frequency vibrational motion of DNA or quasi-harmonic oscillation of a fluorophore within a static DNA structure and are close to diffusive reorganization of a liquid.[32] Computer simulations point out the possibility of relatively large fluctuations in the DNA structure with lifetimes in 100's of picosecond range that is extremely important for DNA−protein interaction and gene regulation.[42,43] The faster time constant of 250 ps may be due to the relaxation of the DNA structure. The longer time constant (13.50 ns) arises from the diffusive motion

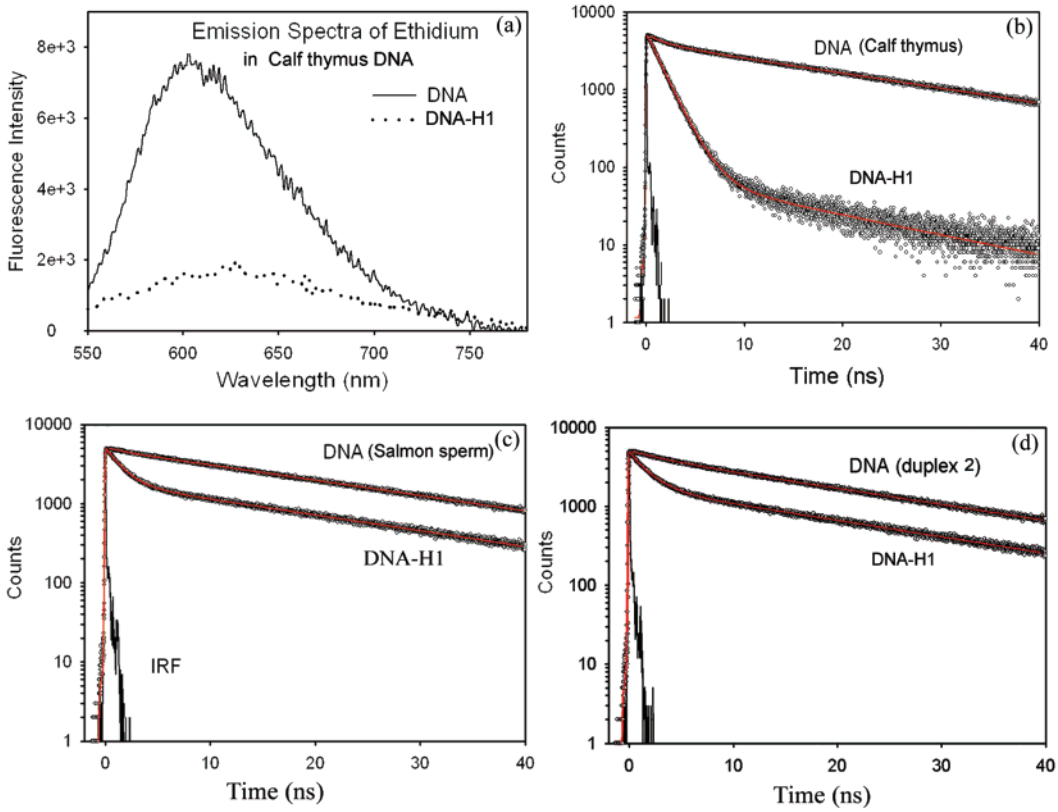

Figure 4. (a) Steady-state emission spectra of EB in calf thymus DNA and DNA−H1 complex are shown. Picosecond resolved fluorescence transients of EB in (b) calf thymus DNA, (c) salmon sperm DNA, and (d) duplex2 and their condensates are shown. Solid lines indicate biexponential numerical fitting of the experimental data points.

Table 1. Time-Resolved Fluorescence Anisotropy of H33258 Bound to the Minor Groove of DNAs and DNA−H1 Complexes

			anisotropy			
DNA type	systems	binding constant (M^{-1})	τ_1 (ns) with %	τ_2 (ns) with %	offset	r_0
calf thymus DNA	DNA	2.63×10^5	0.45(7%)	5.23(32%)	0.17(61%)	0.30
	DNA−H1	5.67×10^5	0.46(3%)	3.86(31%)	0.19(66%)	0.29
salmon sperm DNA	DNA	3.16×10^5	0.45(7%)	5.10(28%)	0.19(65%)	0.29
	DNA−H1	5.44×10^5	0.45(≤1%)	3.64(22%)	0.21(77%)	0.28
duplex1	DNA	2.02×10^8	4.54(82%)		0.06(18%)	0.34
	DNA−H1	2.00×10^8	5.24(44%)		0.19(56%)	0.34

of counterions along the DNA chain and is assigned as δ relaxation.[32,44] The probe H33258 in the DNA−H1 complex shows similar solvation relaxation behavior with time constants of 110 ps and 10.00 ns. The observation is consistent with the fact that the relaxation dynamics of the minor groove at the DNA−H1 interface is similar to that in the minor groove of the DNA without H1.

As evidenced in Figure 2e, H33258 in salmon sperm DNA shows two dynamical time constants of 70 ps and 13.60 ns. The dynamical time constants of H33258 in DNA−H1 are 60 ps and 10.44 ns, which are similar to that of the DNA without H1. The solvation features in the different environments are similar to that in the respective environments of the calf thymus DNA. Structural X-ray crystallographic and NMR studies[14,19] on the ligand with duplex1 show that the specific sequence of (CGCAAATTTGCG) of the DNA is extremely important for the ligand H33258 binding. Solvation dynamics study (Figure 2f) of the ligand bound oligonucleotide reveals two time constants of 60 ps and 8.50 ns. In the duplex1−H1 complex, the time constants change to 120 ps and 25 ns. The observation of slower relaxation dynamics of the probe in the duplex1−H1 complex is not consistent with those in the genomic DNAs. The longer relaxation time (25 ns) may be due to the formation of sandwich like complex of the duplex1 and the protein H1, where the local environment of the probe is more rigid compared to those in genomic DNAs.

The rotational correlation time of H33258 in buffer is 460 ps.[16] The fluorescence anisotropy ($r(t)$) of the probe attached to calf thymus DNA (Figure 3a and Table 1) decays with time constants of 450 ps (7%) and 5.23 ns (33%) with a significant offset (61%) resulting in a persistency of $r(t)$ in our time window (up to 5 ns). The faster time constant of 450 ps is similar to that in bulk buffer and corresponds to the free H33258 population in the solution. We have considered the population to calculate the binding constant of H33258 in the DNA. The binding constants as tabulated in Table 1 are in agreement with the reported values.[45] Relatively longer time constant of ~5 ns may reflect the local reorientational motion of the probe in the minor groove due to bending and torsional motion of the DNA.[46] The slower time constant, which does not decay appreciably in our experimental window, reflects the offset in the measured anisotropy decay and may correspond to the global motion of the DNA. The initial anisotropy (r_0) at $t = 0$ is 0.30 (Table 1). In the DNA−H1 complex, the temporal anisotropy decay of

Table 2. Picosecond Resolved Fluorescence Transients of Ethidium in Various DNAs and Their Condensates with H1

DNA type	systems	binding constant (M^{-1})	τ_1 (ns) with %	τ_2 (ns) with %
calf thymus DNA	DNA	5.30×10^4	1.46(27%)	22.36(73%)
	DNA−H1	4.08×10^2	1.52(98%)	15.34(2%)
salmon sperm DNA	DNA	1.51×10^5	1.14(12%)	22.45(88%)
	DNA−H1	1.08×10^4	1.49(66%)	21.70(34%)
duplex2	DNA	7.74×10^4	3.51(15%)	21.42(85%)
	DNA−H1	3.45×10^3	1.85(65%)	20.83(35%)

the probe reveals a relatively higher offset value that may be due to more geometrical restrictions of the probe in the microenvironment (Figure 3b). The time constants of the fluorescence anisotropy decays of the probe in salmon sperm DNA and in the DNA−H1 complex are tabulated in Table 1. The increased contribution of the offset (77%) in the DNA−H1 complex compared to that in the DNA (65%) reflects higher geometrical restriction on the probe H33258 in the complex. As evidenced in Table 1, the rotational relaxation of the H33258−duplex1 complex is single exponential with a time constant of 6.15 ns with insignificant contribution of residual anisotropy (offset). The observation is consistent with the fact that bending and torsional motion of the duplex1 is comparable to its global tumbling motion. The rigidity of the probe in the duplex1−H1 complex increases significantly as reflected in the $r(t)$ decay revealing a high offset value which does not decay in the experimental time window (up to 5 ns). The observation is also consistent with the formation of the sandwich like duplex1−H1 complex with much higher geometrical restriction on the probe in the complex.

B. Intercalation. In this study, we have used ethidium (EB) as a model intercalator probe ligand, which is a polycyclic aromatic fluorescent dye that intercalates between base pairs of DNA.[47,48] EB displays two types of binding modes to a genomic DNA depending upon the [DNA]:[EB] ratio and ionic strength of the host solution;[49] weak binding at lower [DNA]:[EB] ratio ($K = 4 \times 10^4\ M^{-1}$) and strong binding at higher [DNA]:[EB] ratio ($K = 100 \times 10^4\ M^{-1}$).[11] The probe EB shows significant enhancement of fluorescence intensity and lifetime upon intercalation with DNA (22 ns) compared to that in bulk buffer (1.5 ns). The two lifetime values are so distinct that contribution of the 22 ns component can be used to estimate the relative population of DNA-bound EB and hence to calculate the binding constant[11] of the probe in DNA and the DNA−H1 complex. In order to investigate the change in DNA structure in the DNA−H1 complex, which essentially alters the EB binding in the complex, we have also used EB in our studies.

Figures 4a shows the emission spectra of EB−calf thymus DNA upon interaction with H1. The emission intensity of the intercalated EB is found to be significantly (∼11 times) higher than that of the free EB in bulk buffer.[11] The emission maximum of free EB (630 nm) in bulk buffer shifts toward (25 nm) blue wavelengths in the EB−DNA complex (605 nm).[11] The significant decrease in emission intensity and shift toward red wavelength (622 nm) of EB in the DNA−H1 complex compared to EB−DNA in bulk buffer as evidenced from Figure 4a is indicative of the lessening of the strength of EB binding to the DNA upon complexation with H1. Our observations are consistent with other reports in the literature.[50,51] Picosecond resolved transients of EB−calf thymus DNA complexes are shown in Figure 4b. As shown in Figure 4b the maximum population (22 ns (73%)) of the dye is intercalated to the DNA

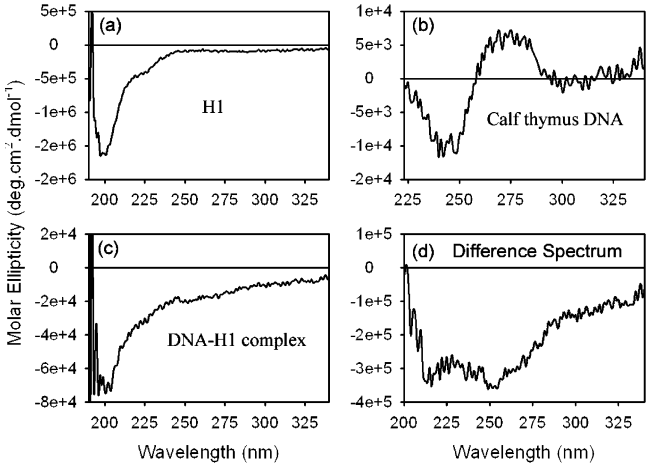

Figure 5. CD spectra of (a) H1, (b) calf thymus DNA in buffer, and (c) calf thymus DNA−H1 complex in buffer. (d) Difference spectra show the structural change of the DNA upon interaction with H1.

in bulk buffer. The transient of EB in the DNA−H1 complex shows that the contribution of a longer ∼22 ns (2%) decay component decreases considerably reflecting significant decrease in the binding affinity of EB in the DNA condensate. The binding constants of EB in the DNA and DNA−H1 complex are shown in Table 2.

In order to investigate the ligand binding of the interspecies DNA−H1 complex, we have studied the complexation of EB−salmon sperm DNA with calf thymus H1. The decrease in fluorescence intensity (data not shown) and change of the contribution of a longer (22ns (34%)) time constant of the EB−DNA−H1 complex (Figure 4c and Table 2) are less than that of the calf thymus DNA condensate. The observation is consistent with the fact that the intercalative interaction of EB with the salmon sperm DNA condensate is much stronger than that with the calf thymus DNA condensate. The stronger interaction in the salmon sperm DNA condensate may be correlated with the less-compact structure of the DNA−H1 complex as evidenced from TEM experiments. In order to study the effect of a base pair sequence in the molecular recognition of the DNA−H1 complex, we choose the oligonucleotide sequence of duplex2. EB strongly intercalates to GC enriched homo oligonucleotides.[52] From Figure 4d and Table 2, it is evident that the perturbation of EB binding (change in 22 ns component) to the duplex2 upon complexation with H1 is less compared to both calf thymus and salmon sperm DNA condensates. From Table 2, it is evident that the faser time constant (∼3.5 ns) of EB in the duplex2 without H1 is slower than that in free buffer (1.5 ns) and much faster than that of the DNA-bound EB through intercalative interaction (22 ns). The time constant may indicate that EB molecules are loosely bound to the DNA through nonintercalative interaction, namely electrostatic binding.[11,49] However, in the duplex2−H1 complex, the loosely bound EB molecules are detached and show a time constant of 1.8 ns similar to that in bulk buffer (1.5 ns).

3. Conformational Study. The conformational change of DNA in the nucleosome core particle and in chromatin has been investigated with great interest by using circular dichroism (CD) spectroscopy.[6,8,53] In a CD spectrum of DNA upon complexation with histones,[6] rotational strength of positive ellipticity at 275 nm significantly decreases, the negative band at 245 nm increases, and both the bands are red-shifted with increasing histone concentration. According to the studies,[54] the change in CD features are consistent with ψ-like conformation of DNA, which remains bound to histone and the remaining linker DNA

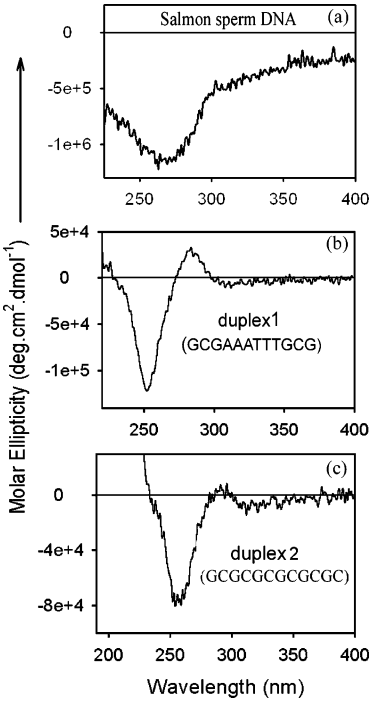

Figure 6. CD difference spectra show the structural change of (a) salmon sperm DNA, (b) duplex1, and (c) duplex2 upon interaction with H1.

has the normal B form. The structural study on mixed conformations of DNA[53] depicts that the exposed or solvent accessible part of a nucleosome remains in the B conformation whereas, the remainder of the base pairs and phosphate backbone, which are covered by histones and protected from solvent, transforms to the C form of DNA.

Figure 5 shows conformational change of calf thymus DNA upon complexation with H1. The CD spectra of free H1 and free DNA in buffer solutions are shown in Figure 5, panels a and b, respectively for comparison. Figure 5c shows the CD spectrum of the DNA−H1 complex. The difference CD spectrum, which is obtained by subtraction of the H1 spectrum from that of the complex, is shown in Figure 5d. A comparison between Figure 5, panels b and d, distinctly reveals the change of DNA structure upon complexation with H1. A negative band at 275 nm is evident from Figure 5d, which indicates the condensed C-form of the DNA in the complex.[53] It should be noted that the condensed DNA structure, which has been measured by CD spectrometry, is not strictly CD spectra but a form of light scattering[55] of left and right circularly polarized light. As evidenced from Figure 6a, the conformational change of salmon sperm DNA in the DNA−H1 complex is similar to that of the calf thymus DNA in the complex. The CD spectrum clearly shows the transformation of DNA from the B to C form. The CD spectroscopic studies as evidenced from Figure 6b show that the degree of condensation of the duplex1 is lesser than that of duplex2 (Figure 6c). Most likely, Figure 6b depicts a mixture of B and C forms in the duplex1−H1 complex.[53] The comparison of the difference CD spectrum of duplex1−H1 (Figure 6c) with those of calf thymus (Figure 5d) and salmon sperm (Figure 6a) DNA molecules also reveals relatively less condensation of duplex1−DNA by H1.

Conclusion

Our studies explore the complexation of DNA molecules with one of the nucleic proteins histone 1 (H1) and its effect on ligand binding to the condensed form of DNA. Transmission electron microscopic (TEM) studies on the structure of the protein−DNA complexes from various sources show that the intraspecies complex (both DNA and protein are from calf thymus) is a compact-globular type, in contrast to the hollow-toroid-type of the interspecies complex (DNA and protein are from salmon sperm and calf thymus, respectively), which is observed for vertibrate sperm cells.[26] Our studies on minor groove binding of H33258 to various kinds of DNA molecules in solution and upon complexation with H1, not only reveal the nature of drug binding in the minor groove but also show the nature of change of the local environments of the DNA molecules in the complex. In the case of genomic DNA molecules, our solvation studies depict an insignificant change in the local environments of DNA molecules upon complexation with H1. Fluorescence anisotropy studies on the minor groove binder H33258 in DNA and in the complex clearly rule out the possibility of detachment of any minor groove-binding drug with the DNA in the complex. In contrast to the minor groove binding, a significant perturbation in the intercalative interaction of EB with various DNA molecules including synthetic oligonucleotide upon complexation with H1 clearly demonstrate that the base-stacking is heavily perturbed in the DNA−H1 complexes. Circular dichroism (CD) studies reveal significant alteration in the conformation of genomic DNA molecules upon complexation with H1, which is consistent with the condensed C form. Perturbation of base stacking as revealed by intercalation of EB could be the consequence of the change in the conformation of the DNA in the complex. These observations are important to understand the binding of drug molecules in the linker DNA of nucleosome core particles.

Acknowledgment. R.S. thanks UGC for the fellowship. We thank DST for a financial grant (SR/FTP/PS-05/2004).

References and Notes

(1) Van Holde, K. *Chromatin*; Springer: New York, 1989.
(2) Hud, N. V. *Biophys. J.* **1995**, *69*, 1355−1362.
(3) Cerritelli, M.; Cheng, N.; Rosenberg, A. H.; McPherson, C. E.; Booy, F. P.; Steven, A. C. *Cell* **1997**, *91*, 271−280.
(4) Plank, C.; Tang, M. X.; Wolfe, A. R.; Szoka, F. C. J. *Hum. Gene Ther.* **1999**, *10*, 319−332.
(5) Rolland, A. *Crit. Rev. Ther. Drug Carrier Syst.* **1998**, *15*, 143−198.
(6) Shih, T. Y.; Fasman, G. D. *Biochemistry* **1972**, *11*, 398−404.
(7) Fasman, G. D.; Schaffhausen, B.; Goldsmith, L.; Adler, A. J. *Biochemistry* **1970**, *9*, 2814−2822.
(8) Gottesfeld, J. M.; Calvin, M.; Cole, R. D.; Igdaloff, D. M.; Moses, V.; Vaughan, W. *Biochemistry* **1972**, *11*, 1422−1430.
(9) McMurray, C. T.; Van Holde, K. E. *Biochemistry* **1991**, *30*, 5631−5643.
(10) Erard, M.; Das, G. C.; de Murcia, G.; Mazen, A.; Pouyet, J.; Champagne, M.; Daune, M. *Nucleic Acids Res.* **1979**, *6*, 3231−3253.
(11) Sarkar, R.; Pal, S. K. *Biopolymers* **2006**, *83*, 675−686.
(12) Quigley, G. J.; Wang, A. J. H.; Ughetto, G.; Marel, G. V. D.; Van Boom, J. H.; Rich, A. *Proc. Natl. Acad. Sci. U.S.A.* **1980**, *77*, 7204−7208.
(13) Soderlind, K. J.; Gorodetsky, B.; Singh, A.; Bachur, N.; Miller, G.; Lown, J. W. *Anti-Cancer Drug. Des.* **1999**, *14*, 19−36.
(14) Vega, M. C.; Garcia Saez, I.; Aymami, J.; Eritja, R.; Van Der Marel, G. A.; Van Boom, J. H.; Rich, A.; Coll, M. *Eur. J. Biochem.* **1994**, *222*, 721−726.
(15) Pal, S. K.; Zhao, L.; Zewail, A. H. *Proc. Natl. Acad. Sci. U.S.A.* **2003**, *100*, 8113−8118.
(16) Banerjee, D.; Pal, S. K. *Chem. Phys. Lett.* **2006**, *432*, 257−262.
(17) Jin, R.; Breslauer, K. J. *Proc. Natl. Acad. Sci. U.S.A.* **1988**, *85*, 8939−8942.
(18) Vardevanian, P. O.; Antonian, A. P.; Davtian, A. G.; Arakelian, A. V.; Minasian, S. G.; Tavadian, L. A. *Biofizika* **2005**, *50*, 371−373.
(19) Parkinson, J. A.; Ebrahimi, S. E.; McKie, J. H.; Douglas, K. T. *Biochemistry* **1994**, *33*, 8442−8452.
(20) Sheffield, V. C.; Cox, D. R.; Lerman, L. S.; Myers, R. M. *Proc. Natl. Acad. Sci. U.S.A.* **1989**, *86*, 232−236.

(21) Gallagher, S. R. In *Current Protocols in Molecular Biology*; Ausubel, F. M., Brent, R., Kingston, K. E., Moore, D. D., Seidman, J. G., Smith, J. A., Struhl, K., Eds.; Greene and Wiley-Interscience: New York, 1994.
(22) Cosa, G.; Focsaneanu, K.-S.; McLean, J. R. N.; McNamee, J. P.; Scaiano, J. C. *Photochem. Photobiol.* **2001**, *73*, 585−599.
(23) Horng, M. L.; Gardecki, J. A.; Papazyan, A.; Maroncelli, M. *J. Phys. Chem.* **1995**, *99*, 17311−17337.
(24) Lakowicz, J. R. *Principles of Fluorescence Spectroscopy*; Kluwer Academic/Plenum: New York, 1999.
(25) O'Connor, D. V.; Philips, D. *Time Correlated Single Photon Counting*; Academic Press: London, 1984.
(26) Hud, N. V.; Allen, M. J.; Downing, K. H.; Lee, J.; Balhorn, R. *Biochem. Biophys. Res. Commun.* **1993**, *193*, 1347−1354.
(27) Bottcher, C.; Endisch, C.; Fuhrhop, J.-H.; Catterall, C.; Eaton, M. *J. Am. Chem. Soc.* **1998**, *120*, 12−17.
(28) Tanaka, K.; Okahata, Y. *J. Am. Chem. Soc.* **1996**, *118*, 10679−10683.
(29) Conwell, C. C.; Vilfan, I. D.; Hud, N. V. *Proc. Natl. Acad. Sci. U.S.A.* **2003**, *100*, 9296−9301.
(30) Saito, M.; Kobayashi, M.; Iwabuchi, S.; Morita, Y.; Takamura, Y.; Tamiya, E. *J. Biochem. (Tokyo)* **2004**, *136*, 813−823.
(31) Pal, S. K.; Zewail, A. H. *Chem. Rev.* **2004**, *104*, 2099−2124.
(32) Brauns, E. B.; Madaras, M. L.; Coleman, R. S.; Murphy, C. J.; Berg, M. A. *J. Am. Chem. Soc.* **1999**, *121*, 11644−11649.
(33) Andreatta, D.; Perez Lustres, J. L.; Kovalenko, S. A.; Ernsting, N. P.; Murphy, C. J.; Coleman, R. S.; Berg, M. A. *J. Am. Chem. Soc.* **2005**, *127*, 7270−7271.
(34) Sen, S.; Gearheart, L. A.; Rivers, E.; Liu, H.; Coleman, R. S.; Murphy, C. J.; Berg, M. A. *J. Phys. Chem. B* **2006**, *110*, 13248−13255.
(35) Somoza, M. M.; Andreatta, D.; Murphy, C. J.; Coleman, R. S.; Berg, M. A. *Nucleic Acids Res.* **2004**, *32*, 2494−2507.
(36) Brauns, E. B.; Madaras, M. L.; Coleman, R. S.; Murphy, C. J.; Berg, M. A. *Phys. Rev. Lett.* **2002**, *88*, 158101.
(37) Edwards, K. J.; Brown, D. G.; Spink, N.; Skelly, J. V.; Neidle, S. *J. Mol. Biol.* **1992**, *226*, 1161−1173.
(38) Sarkar, R.; Ghosh, M.; Shaw, A. K.; Pal, S. K. *J. Photochem. Photobiol., B* **2005**, *79*, 67−78.
(39) Sarkar, R.; Ghosh, M.; Pal, S. K. *J. Photochem. Photobiol. B: Biol.* **2005**, *78*, 93−98.
(40) Majumder, P.; Sarkar, R.; Shaw, A. K.; Chakraborty, A.; Pal, S. K. *J. Colloid Interface Sci.* **2005**, *290*, 462−474.
(41) Fee, R. S.; Maroncelli, M. *Chem. Phys.* **1994**, *183*, 235−247.
(42) Beveridge, D. L.; Ravishanker, G. *Curr. Opin. Struct. Biol.* **1994**, *4*, 246−255.
(43) Young, M. A.; Ravishanker, G.; Beveridge, D. L. *Biophys. J.* **1997**, *73*, 2313−2336.
(44) Saif, B.; Mohr, R. K.; Montrose, C. J.; Litovitz, T. A. *Biopolymers* **1991**, *31*, 1171−1180.
(45) Bostock-Smith, C. E.; Searle, M. S. *Nucleic Acids Res.* **1999**, *27*, 1619−1624.
(46) Millar, D. P.; Robbins, R. J.; Zewail, A. H. *J. Chem. Phys.* **1982**, *76*, 2080−2094.
(47) Tsai, C. C.; Jain, S. C.; Sobell, H. M. *Proc. Natl. Acad. Sci. U.S.A.* **1975**, *72*, 628−632.
(48) Breslauer, K. J.; Remeta, D. P.; Chou, W. Y.; Ferrante, R.; Curry, J.; Zaunczkowski, D.; Snyder, J. G.; Marky, L. A. *Proc. Natl. Acad. Sci. U.S.A.* **1987**, *84*, 8922−8926.
(49) Vardevanyan, P. O.; Antonyan, A. P.; Parsadanyan, M. A.; Davtyan, H. G.; Karapetyan, A. T. *Exp. Mol. Med.* **2003**, *35*, 527−533.
(50) Olins, D. E. *J. Mol. Biol.* **1969**, *43*, 439−460.
(51) Chitre, A. V.; Korgaonkar, K. S. *Biochem. J.* **1979**, *179*, 213−219.
(52) Krugh, T. R.; Wittlin, F. N.; Cramer, S. P. *Biopolymers* **1975**, *14*, 197−210.
(53) Johnson, R. S.; Chan, A.; Hanlon, S. *Biochemistry* **1972**, *11*, 4347−4358.
(54) Cowman, M. K.; Fasman, G. D. *Proc. Natl. Acad. Sci. U.S.A.* **1978**, *75*, 4759−4763.
(55) Rodger, A.; Norden, B. *Circular Dichroism and Linear Dichroism*; Oxford University Press: Oxford, 1997.

BM700690P